# Boulder height – exposure age relationships from a global glacial $^{10}$Be compilation

Jakob Heyman[1]*, Patrick J. Applegate[2], Robin Blomdin[3], Natacha Gribenski[3], Jonathan M. Harbor[3,4], Arjen P. Stroeven[3]

1. Department of Earth Sciences, University of Gothenburg, Sweden
2. Earth and Environmental Sciences Institute, Pennsylvania State University, USA
3. Geomorphology and Glaciology, Department of Physical Geography and Bolin Centre for Climate Research, Stockholm University, Sweden
4. Department of Earth, Atmospheric, and Planetary Sciences, Purdue University, USA

* jakob.heyman@gu.se

## $^{10}$Be exposure age calculation

To calculate $^{10}$Be exposure ages we use a modified version of the CRONUS calculator code (Balco et al., 2008), using the nuclide-specific LSD scaling of Lifton et al. (2014) and the muon parameterization of Phillips et al. (2016a). The general calculation procedure is similar to the CRONUS calculator, using numerical integration over time of the $^{10}$Be production adjusted for sample thickness, topographic shielding, $^{10}$Be decay, and erosion.

Main calculator characteristics:

- Nuclide-specific LSD spallation and muon $^{10}$Be production rate scaling based on simulated cosmic ray fluxes (Lifton et al. 2014).
- Time-dependent spallation $^{10}$Be production rate with reference production rate: 3.98 ± 0.17 atoms $g^{-1}$ $yr^{-1}$ based on 22 $^{10}$Be production rate calibration sites (see below).
- Time-constant muon $^{10}$Be production rate parameterization based on Antarctica depth profile data (Phillips et al. 2016a).
- Muon production depth dependence for samples with an assumed erosion rate based on the Phillips et al. (2016a) parameterization. Because we calculate zero erosion exposure ages, this only applies for the production rate calibration sites with assumed constant erosion rates (see Supplementary Dataset).
- Adjustment of the time-dependent production rate to the year of sampling (assuming a constant production since 2010).
- Atmospheric pressure based on sample elevation and ERA-40 re-analysis dataset (Uppala et al. 2005).
- Attenuation length for calculating the spallation production rate adjustments for sample thickness and erosion rate interpolated from atmospheric pressure and cutoff rigidity (Marrero et al. 2016).
- $^{10}$Be half-life: 1.387 Ma (Chmeleff et al. 2010; Korschinek et al. 2010).
- Standardization of all $^{10}$Be concentrations to the 07KNSTD standard (Nishiizumi et al. 2007).

The exposure age calculator code (Octave/Matlab) is included as supplementary material.

**$^{10}$Be reference production rate calibration**

To derive a reference $^{10}$Be production rate we have compiled recently published data (2009-2016) and re-calibrated reference $^{10}$Be production rates for 25 individual sites around the world (Fig. 1a) with a minimum of three individual samples per calibration site. For samples with multiple $^{10}$Be measurements (repeat measurements of one sample or measurements of multiple samples from the same surface) we calculate uncertainty-weighted mean $^{10}$Be concentrations and uncertainties. To account for measurement uncertainties, we use the higher of the reported (or calculated uncertainty-weighted for multiple measurements) $^{10}$Be concentration uncertainty and 2.9% of the $^{10}$Be concentration, based on the inter-laboratory comparison reported by Jull et al. (2015). We generally follow published assumptions on the exposure history, and we use published sample density and erosion rates. In the absence of sampling year information we assume that sampling occurred two years before publication. We adjust all calibration ages to year before sampling and we re-calibrate radiocarbon-based calibration ages using OxCal 4.2 (Bronk Ramsey 2009) and the IntCal13, Marine13 (Reimer et al. 2013), and the SHCal13 (Hogg et al. 2013) calibration curves.

To calibrate the site reference $^{10}$Be production rates, we calculate exposure ages for each sample from a site with the calculator described above and adjust the reference $^{10}$Be production rate to derive the best match between the exposure ages and the central calibration age using chi square minimization. Because the calibration age uncertainty is not an independent variable for each sample, we add the calibration age uncertainty in quadrature to the reference production rate using standard error propagation.

To minimize the risk of prior and incomplete exposure (Heyman et al. 2011) affecting the production rate calibration, we require very well-clustered sample exposure ages yielding a reduced chi square value $\chi^2_R$ < 1.5 (calculated against the central calibration age and not including the calibration age uncertainty). Using a constant cut-off value honors the group size (number of samples per calibration site), with the probability of getting values <1.5 increasing with group size assuming the exposure age scatter is caused only by the measurement uncertainty (Fig. S2). For calibration sites yielding $\chi^2_R \geq 1.5$, a maximum of 1/3 of the samples have been excluded as outliers (still requiring a minimum of three individual samples) to achieve $\chi^2_R < 1.5$. For calibration sites that do not fulfill the $\chi^2_R < 1.5$ criterion we use the full set of samples to calculate a reference production rate but these production rates are not included in the global average reference production rate because excessive internal scatter indicates the undue importance of prior and/or incomplete exposure.

The site reference $^{10}$Be production rates range from 3.54 ± 0.14 atoms g$^{-1}$ yr$^{-1}$ to 4.93 ± 0.17 atoms g$^{-1}$ yr$^{-1}$ (Fig. S1; Supplementary Dataset). Two sites (sites 24 and 25) cannot fulfill the $\chi^2_R < 1.5$ criterion and are therefore excluded from further analysis. Of the remaining 23 site reference production rates, site 2 has a significantly higher reference production rate than all other site reference production rates with no overlap within 2σ. With both Peirce's (1852) and Chauvenet's (1863) criteria the reference production rate of site 2 is identified as an outlier, and we therefore exclude it from further analysis. The arithmetic mean and standard deviation of the remaining 22 reference production rates yields a tightly clustered reference $^{10}$Be production rate of 3.98 ± 0.17 atoms g$^{-1}$ yr$^{-1}$ (Fig. S1) which is used as a global average in the exposure age calculator described above.

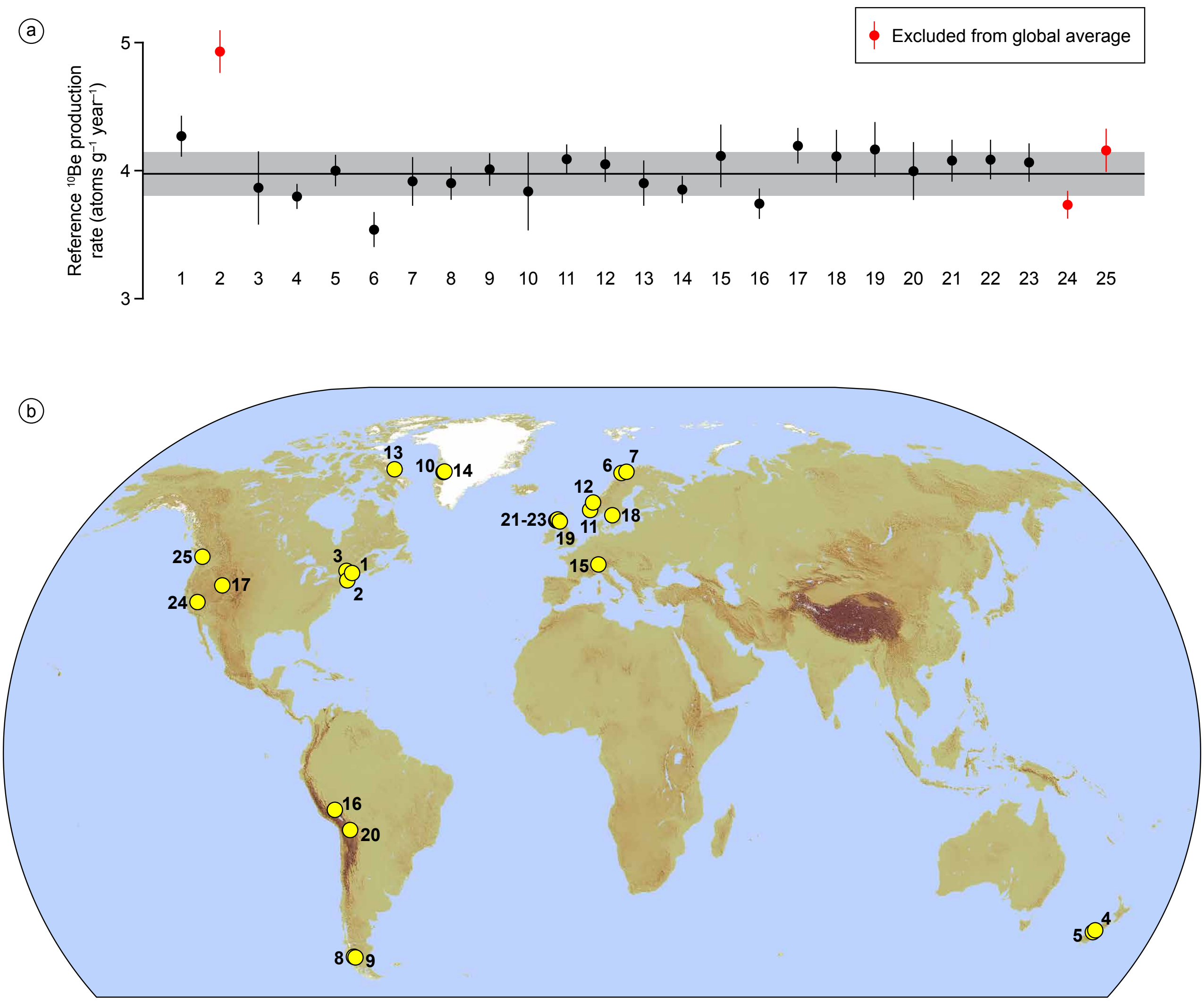


**Figure S1.** (a) Calibrated site reference $^{10}$Be production rates and global average and 1σ uncertainty range (horizontal black line and grey band). The production rates of sites 24 and 25 are excluded from the global average because internal scatter was deemed too large ($\chi^2_R \geq 1.5$). The production rate of site 2 is excluded from the global average because it is identified as an outlier with both Peirce's (1852) and Chauvenet's (1863) criteria. See Supplementary Dataset for sample and site data. (b) Map showing the location of the 25 $^{10}$Be production rate calibration sites.

Calibration site publications:

| | | | |
|---|---|---|---|
| 1: | Balco et al. (2009), Borchers et al. (2016) | 14: | Young et al. (2013) |
| 2-3: | Balco et al. (2009) | 15: | Claude et al. (2014) |
| 4-5: | Putnam et al. (2010) | 16: | Kelly et al. (2015), Phillips et al. (2016b) |
| 6-7: | Fenton et al. (2011) | 17: | Lifton et al. (2015) |
| 8-9: | Kaplan et al. (2011) | 18: | Stroeven et al. (2015) |
| 10: | Briner et al. (2012), Young et al. (2013) | 19: | Small and Fabel (2015) |
| 11-12: | Goehring et al. (2012) | 20: | Martin et al. (2015) |
| 13: | Balco et al. (2009), Young et al. (2013) | 21-25: | Borchers et al. (2016) |

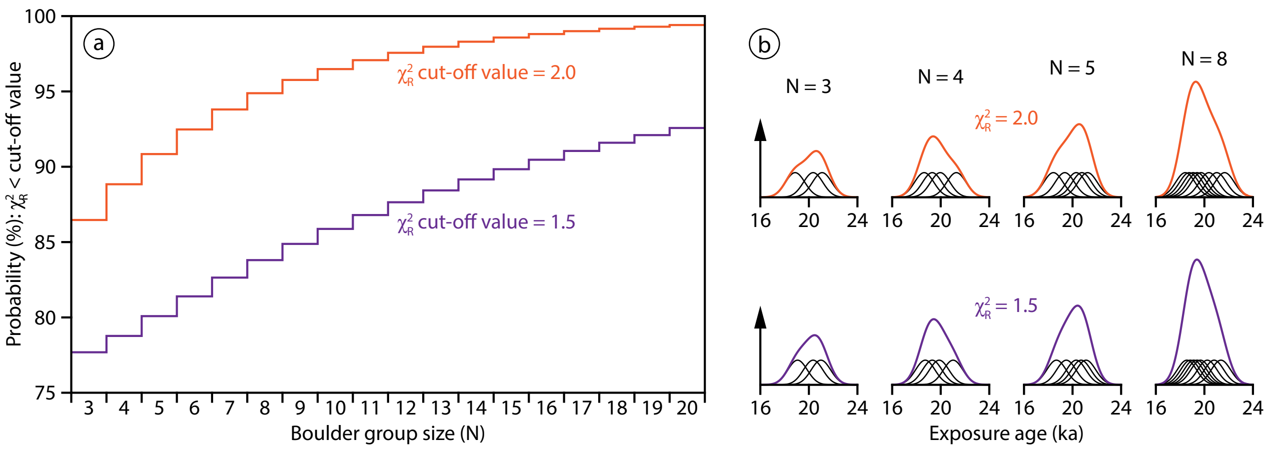


**Figure S2.** (a) Theoretical probability for getting a reduced chi-square value $\chi^2_R < 2.0$ (criterion for well-clustered boulder groups) and $\chi^2_R < 1.5$ (criterion for well-clustered reference $^{10}Be$ production rates). Using a constant cut-off value honors the group size as the theoretical probability of fulfilling the clustering criterion increases with group size. (b) Examples of individual sample and summed probability density distributions for groups of 3/4/5/8 samples yielding $\chi^2_R = 2.0$ and $\chi^2_R = 1.5$.

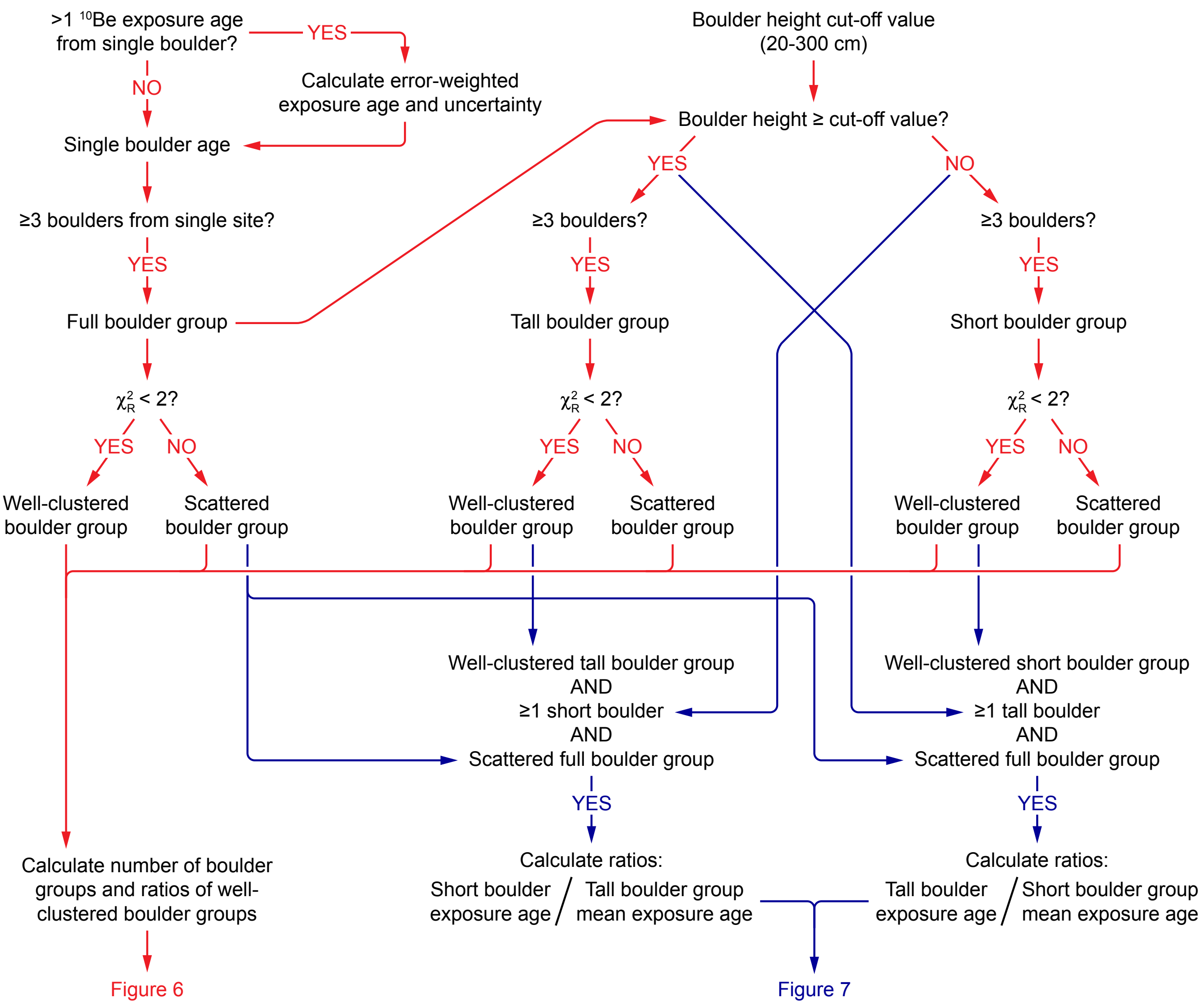


**Figure S3.** Flowchart for the data analysis of boulder group exposure age clustering and boulder height yielding the data for Figures 6 and 7 in the main article.

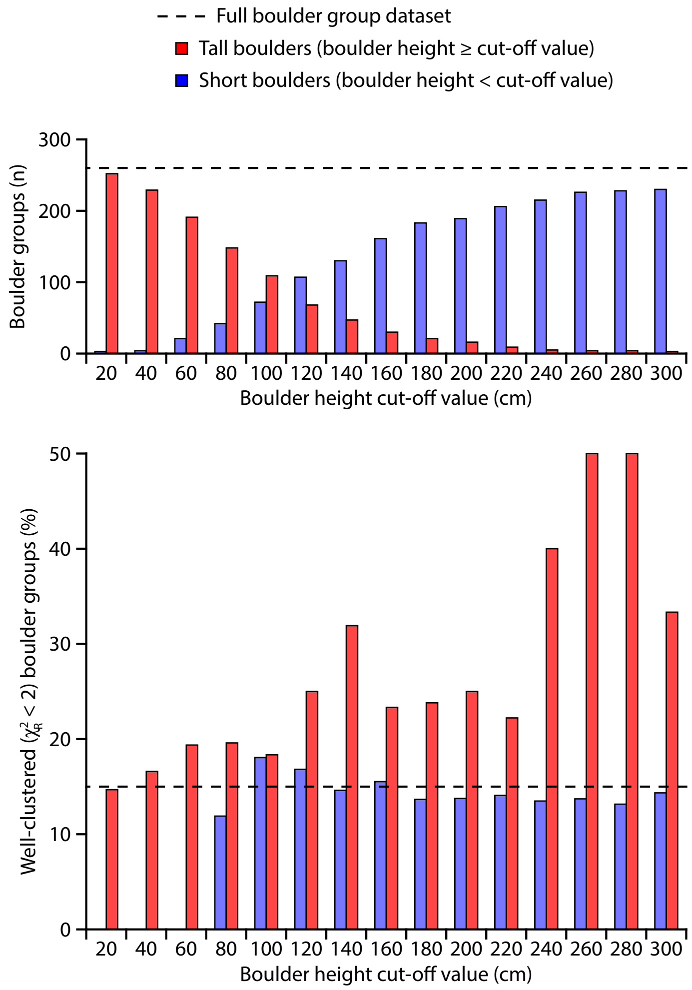


**Figure S4.** Number of boulder groups with a minimum of five individual boulders (upper graph) and fraction of well-clustered exposure age groups (lower graph) for tall (red) and short (blue) boulder groups defined by boulder height cut-off values ranging from 20 cm to 300 cm. The horizontal dashed lines show the full number of boulder groups (upper graph) and the fraction of well-clustered boulder groups of the full boulder group dataset (lower graph).

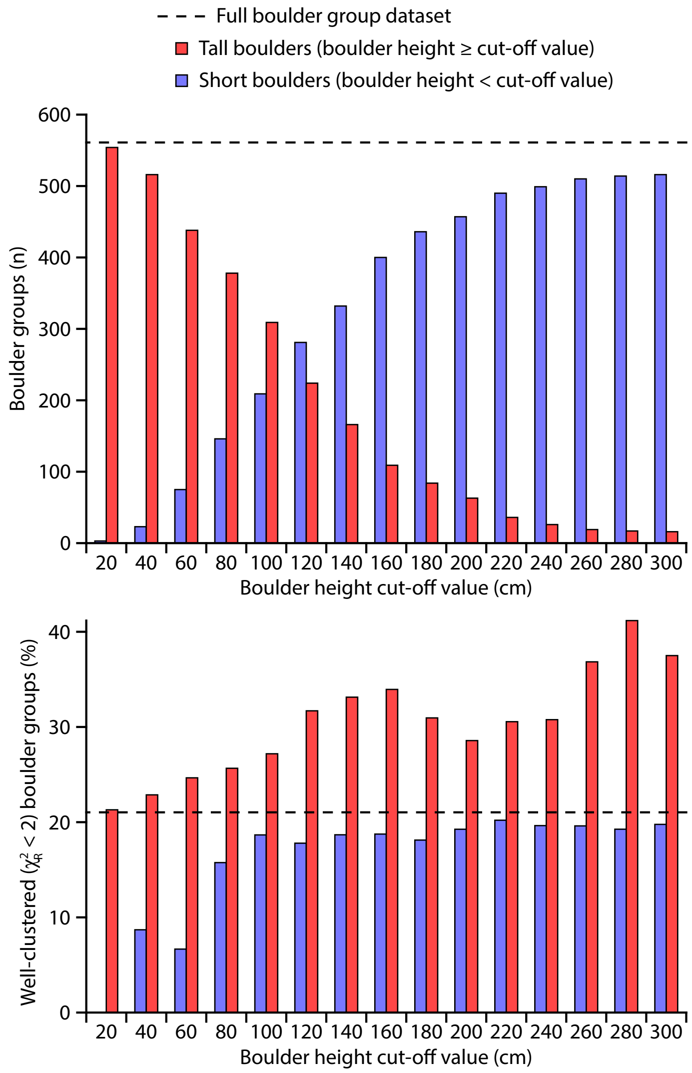


**Figure S5.** Number of boulder groups, excluding cobble samples, with a minimum of three individual boulders (upper graph) and fraction of well-clustered exposure age groups (lower graph) for tall (red) and short (blue) boulder groups defined by boulder height cut-off values ranging from 20 cm to 300 cm. The horizontal dashed lines show the full number of boulder groups (upper graph) and the fraction of well-clustered boulder groups of the full boulder group dataset (lower graph).

**References**

Balco G, Stone JO, Lifton NA, Dunai TJ, 2008. A complete and easily accessible means of calculating surface exposure ages or erosion rates from $^{10}Be$ and $^{26}Al$ measurements. Quaternary Geochronology 3, 174-195.

Balco G, Briner J, Finkel RC, Rayburn JA, Ridge JC, Schaefer JM, 2009. Regional beryllium-10 production rate calibration for late-glacial northeastern North America. Quaternary Geochronology 4, 93-107.

Borchers B, Marrero S, Balco G, Caffee M, Goehring B, Lifton N, Nishiizumi K, Phillips F, Schaefer J, Stone J, 2016. Geological calibration of spallation production rates in the CRONUS-Earth project. Quaternary Geochronology 31, 188-198.

Briner JP, Young NE, Goehring BM, Schaefer JM, 2012. Constraining Holocene $^{10}Be$ production rates in Greenland. Journal of Quaternary Science 27, 2-6.

Bronk Ramsey C, 2009. Bayesian analysis of radiocarbon dates. Radiocarbon 51, 337-360.

Chauvenet W, 1863. A manual of spherical and practical astronomy, Vol II.

Chmeleff J, von Blanckenburg F, Kossert K, Jakob D, 2010. Determination of the $^{10}Be$ half-life by multicollector ICP-MS and liquid scintillation counting. Nuclear Instruments and Methods in Physics Research B 268, 192-199.

Claude A, Ivy-Ochs S, Kober F, Antognini M, Salcher B, Kubik PW, 2014. The Chironico landslide (Valle Leventina, southern Swiss Alps): age and evolution. Swiss Journal of Geoscience 107, 273-291.

Fenton CR, Hermanns RL, Blikra LH, Kubik PW, Bryant C, Niedermann S, Meixner A, Goethals MM, 2011. Regional $^{10}Be$ production rate calibration for the past 12 ka deduced from the radiocarbon-dated Grøtlandsura and Russenes rock avalanches at 69° N, Norway. Quaternary Geochronology 6, 437-452.

Goehring BM, Lohne ØS, Mangerud J, Svendsen JI, Gyllencreutz R, Schaefer J, Finkel R, 2012. Late glacial and Holocene $^{10}Be$ production rates for western Norway. Journal of Quaternary Science 27, 89-96.

Heyman J, Stroeven AP, Harbor JM, Caffee MW, 2011. Too young or too old: evaluating cosmogenic exposure dating based on an analysis of compiled boulder exposure ages. Earth and Planetary Science Letters 302, 71-80.

Hogg AG, Hua Q, Blackwell PG, Niu M, Buck CE, Guilderson TP, Heaton TJ, Palmer JG, Reimer PJ, Reimer RW, Turney CSM, Zimmerman SRH, 2013. SHCal13 Southern Hemisphere calibration, 0-50,000 years cal BP. Radiocarbon 55, 1889-1903.

Jull AJT, Scott EM, Bierman P, 2015. The CRONUS-Earth inter-comparison for cosmogenic isotope analysis. Quaternary Geochronology 26, 3-10.

Kaplan MR, Strelin JA, Schaefer JM, Denton GH, Finkel RC, Schwartz R, Putnam AE, Vandergoes MJ, Goehring BM, Travis SG, 2011. In-situ cosmogenic $^{10}Be$ production rate at Lago Argentino, Patagonia: implications for late-glacial climate chronology. Earth and Planetary Science Letters 309, 21-32.

Kelly MA, Lowell TV, Applegate PJ, Phillips FM, Schaefer JM, Smith CA, Kim H, Leonard KC, Hudson AM, 2015. A locally calibrated, late glacial $^{10}Be$ production rate from a low-latitude, high-altitude site in the Peruvian Andes. Quaternary Geochronology 26, 70-85.

Korschinek G, Bergmaier A, Faestermann T, Gerstmann UC, Knie K, Rugel G, Wallner A, Dillmann I, Dollinger G, von Gostomski CL, Kossert K, Maiti M, Poutivtsev M, Remmert A, 2010. A new value for the half-life of $^{10}Be$ by heavy-ion elastic recoil detection and liquid scintillation counting. Nuclear Instruments and Methods in Physics Research B 268, 187-191.

Lifton N, Sato T, Dunai TJ, 2014. Scaling in situ cosmogenic nuclide production rates using analytical approximations to atmospheric cosmic-ray fluxes. Earth and Planetary Science Letters 386, 149-160.

Lifton N, Caffee M, Finkel R, Marrero S, Nishiizumi K, Phillips FM, Goehring B, Gosse J, Stone J, Schaefer J, Theriault B, Jull AJT, Fifield K, 2015. In situ cosmogenic nuclide production rate calibration for the CRONUS-Earth project from Lake Bonneville, Utah, shoreline features. Quaternary Geochronology 26, 56-69.

Marrero SM, Phillips FM, Borchers B, Lifton N, Aumer R, Balco G, 2016. Cosmogenic nuclide systematics and the CRONUScalc program. Quaternary Geochronology 31, 160-187.

Martin LCP, Blard P-H, Lavé J, Braucher R, Lupker M, Condom T, Charreau J, Mariotti V, Arnold M, Aumaître G, Bourlès DL, Keddadouche K, Davy E, 2015. In situ cosmogenic $^{10}$Be production rate in the high tropical Andes. Quaternary Geochronology 30, 54-68.

Nishiizumi K, Imamura M, Caffee MW, Southon JR, Finkel RC, McAninch J, 2007. Absolute calibration of $^{10}$Be AMS standards. Nuclear Instruments and Methods in Physics Research B 258, 403-413.

Peirce B, 1852. Criterions for the rejection of doubtful observations. Astronomical Journal 2, 161-163.

Phillips FM, Argento DC, Balco G, Caffee MW, Clem J, Dunai TJ, Finkel R, Goehring B, Gosse JC, Hudson AM, Jull AJT, Kelly MA, Kurz M, Lal D, Lifton N, Marrero SM, Nishiizumi K, Reedy RC, Schaefer J, Stone JOH, Swanson T, Zreda MG, 2016a. The CRONUS-Earth project: a synthesis. Quaternary Geochronology 31, 119-154.

Phillips FM, Kelly MA, Hudson AM, Stone JOH, Schaefer J, Marrero SM, Fifield LK, Finkel R, Lowell T, 2016b. CRONUS-Earth calibration samples from the Huancané II moraines, Quelccaya ice cap, Peru. Quaternary Geochronology 31, 220-236.

Putnam AW, Schaefer JM, Barrell DJA, Vandergoes M, Denton GH, Kaplan MR, Finkel RC, Schwartz R, Goehring BM, Kelley SE, 2010. In situ cosmogenic $^{10}$Be production-rate calibration from the Southern Alps, New Zealand. Quaternary Geochronology 5, 392-409.

Reimer PJ, Bard E, Bayliss A, Beck JW, Blackwell PG, Bronk Ramsey C, Buck CE, Cheng H, Edwards RL, Friedrich M, Grootes PM, Guilderson TP, Haflidason H, Hajdas I, Hatté C, Heaton TJ, Hoffmann DL, Hogg AG, Hughen KA, Kaiser KF, Kromer B, Manning SW, Niu M, Reimer RW, Richards DA, Scott EM, Southon JR, Staff RA, Turney CSM, van der Plicht J, 2013. IntCal13 and Marine13 radiocarbon age calibration curves 0-50,000 years cal BP. Radiocarbon 55, 1869-1887.

Small D, Fabel D, 2015. A Lateglacial $^{10}$Be production rate from glacial lake shorelines in Scotland. Journal of Quaternary Science 30, 509-513.

Stroeven AP, Heyman J, Fabel D, Björck S, Caffee MW, Fredin O, Harbor JM, 2015. A new Scandinavian reference $^{10}$Be production rate. Quaternary Geochronology 29, 104-115.

Uppala SM, Kållberg PW, Simmons AJ, Andrae U, da Costa Bechtold Fiorino M, Gibson JK, Haseler J, Hernandez A, Kelly GA, Li X, Onogi K, Saarinen S, Sokka N, Allan RP, Andersson E, Arpe K, Balmaseda MA, Beljaars ACM, van de Berg L, Bidlot J, Bormann N, Caires S, Chevallier F, Dethof A, Dragosavac M, Fisher M, Fuentes M, Hagemann S, Hólm E, Hoskins BJ, Isaksen L, Janssen PAEM, Jenne R, McNally AP, Mahfouf J-F, Morcrette J-J, Rayner NA, Saunders RW, Simon P, Sterl A, Trenberth KE, Untch A, Vasiljevic D, Viterbo P, Woollen J, 2005. The ERA-40 re-analysis. Quarterly Journal of the Royal Meteorological Society 131, 2961-3012.

Young NE, Schaefer JM, Briner JP, Goehring BM, 2013. A $^{10}$Be production-rate calibration for the Arctic. Journal of Quaternary Science 28, 515-526.